RSC Advances

PAPER

View Article Online
View Journal | View Issue

Cite this: *RSC Adv.*, 2023, **13**, 2756

Synthesis of an amantadine-based novel Schiff base and its transition metal complexes as potential ALP, α-amylase, and α-glucosidase inhibitors†

Aliya Ajaz,[a] Muhammad Ashraf Shaheen,*[a] Maqsood Ahmed,[b] Khurram Shahzad Munawar,[ac] Abu Bakar Siddique,[a] Abdul Karim,[a] Nazir Ahmad[d] and Muhammad Fayyaz ur Rehman*[a]

A Schiff base ligand HL, (*E*)-2-((adamantan-1-ylimino)methyl)-6-allylphenol, was synthesized by condensation of amantadine with 3-allyl-2-hydroxybenzaldehyde, followed by the synthesis of its Zn(II), Co(II), Cr(III), and VO(IV) complexes under reflux conditions. The synthesized compounds were comprehensively elucidated by using different spectroscopic and analytical techniques: UV-Vis, ^{1}H and ^{13}C-NMR, FT-IR, ESI-MS, thermal, and single-crystal XRD analysis. The chemical composition of the synthesized compounds was also verified by molar conductance and elemental analysis. An octahedral geometry for Cr(III) and Co(II) complexes, tetrahedral for Zn(II) complex, and square pyramidal geometry have been proposed for VO(IV) complexes. The antidiabetic activities of the synthesized compounds were also evaluated by performing *in vitro* α-amylase and α-glucosidase inhibition studies. The Co(II) complex exhibited the highest α-glucosidase inhibitory activity, whereas oxovanadium(IV) and zinc(II) complexes were also found to be effective against α-amylase. In alkaline phosphatase (ALP) inhibition studies, the HL was found to be inactive, while the complexes showed remarkable enzyme inhibition in the following order: VO > Zn > Co, in a concentration-dependent manner.

Received 6th November 2022
Accepted 9th January 2023

DOI: 10.1039/d2ra07051k

rsc.li/rsc-advances

Introduction

Schiff bases have a significant role as chelating ligands, as these can easily form stable colored complexes with transition metals when stabilizing, and highly supportive groups like –OH are present close to the imine (–HC=N–) group.[1,2] In recent years, the coordination modes of Schiff base ligands to transition metal ions have been studied comprehensively in the pharmaceutical industry.[3] Several substituted heterocyclic moieties in coordination with transition metal ions have shown improved pharmacological and physio-chemical properties.[4] Therefore, these compounds have been evaluated as effective anticancer, herbicidal, antibacterial, antifungal, antioxidant, and anti-proliferative agents.[5] Several transition metal complexes based on the ONNO Schiff base are reported as potential antibacterial and antifungal agents.[6] Schiff base complexes of Cr(III), Mn(II), Zn(II), and Co(II) have shown significant antimicrobial, anticancer, and antidiabetic activities.[7–10]

Diabetes mellitus (DM) is a metabolic disorder resulting in high blood glucose levels due to the lack of insulin or the inability of insulin to perform glucose metabolism.[11,12] Diabetes can be controlled by reducing glucose absorption by inhibiting enzymes involved in the digestion of carbohydrates. The α-glucosidase and α-amylase are the main enzymes involved in the breakdown of carbohydrates and the digestion of lipids. α-Amylase is involved in the digestion of carbohydrates, while α-glucosidase is involved in the digestion of starch and disaccharides into glucose.[13] These enzymes can be suppressed by effective inhibitors to treat diabetes.[14] A large number of coordinated compounds such as chromium, cobalt, zinc, vanadium, tungsten, and molybdenum have been used in the remediation of diabetes.[15–17] Metformin-Schiff base complexes with oxovanadium(IV) have shown strong antidiabetic effects,[18] whereas Zn(II) Schiff base complexes have shown improved α-glucosidase inhibition.[19] Alkaline phosphatase (ALP) is an enzyme that causes hydrolysis under alkaline conditions and recycles phosphate in living cells.[20] Several metal complexes of Schiff bases are potent ALP inhibitors, causing the deactivation of the enzyme.[21] Some oxovanadium complexes of triazole Schiff bases

[a]*Institute of Chemistry, University of Sargodha, 40100, Pakistan. E-mail: aliyarajput2822@gmail.com; ashraf.shaheen@uos.edu.pk; fayyaz9@gmail.com; abubakar.siddique@uos.edu.pk; abdul.karim@uos.edu.pk*

[b]*Materials Chemistry Laboratory, Institute of Chemistry, The Islamia University of Bahawalpur, Baghdad-ul-Jadeed Campus 63100, Pakistan. E-mail: maqsood.ahmed@iub.edu.pk*

[c]*Department of Chemistry, University of Mianwali, Mianwali, 42200, Pakistan. E-mail: khurramchemist@gmail.com*

[d]*Department of Chemistry, Government College University Lahore, Lahore 54000, Pakistan. E-mail: nazirphysical@gmail.com*

† Electronic supplementary information (ESI) available. CCDC 2231982 and 2231983. For ESI and crystallographic data in CIF or other electronic format see DOI: https://doi.org/10.1039/d2ra07051k

exhibited excellent alkaline inhibition and anti-diabetic properties.[22,23] Zinc(II) complexes of thiones and coordinated cobalt complexes have also been explored for alkaline phosphatase inhibition.[24,25]

In view of these findings, we decided to synthesize amantadine-based Schiff base and its transition metal complexes. Adamantane-based derivatives are already known for their medicinal properties as antiviral, antiparkinsonian, antimicrobial, anticancer agents, and antidiabetic agents.[26–32] Nowadays, the adamantine ($C_{10}H_{16}$) moiety is being introduced into a skeleton of active drugs to improve their lipophilic character and pharmacological properties.[33–35] Several metal complexes of amantadine-based ligands have been synthesized and have already been described in the literature. Platinum(II) and platinum(IV) complexes with amantadine are known because of their biological importance as effective anticancer agents.[36] The silver complexes with amantadine and memantine have been reported as effective antibacterial agents against Gram-positive and Gram-negative strains.[37] Following this lead, we synthesized a novel amantadine-based ligand by condensing 3-allyl-2-hydroxybenzaldehyde with amantadine and performing complexation with various metals. The structures of the synthesized compounds were investigated by means of FT-IR, MS, NMR (^{1}H and ^{13}C), UV-Vis, thermal, and elemental analysis. The three-dimensional structure was elucidated by the single crystal X-ray diffraction (SC-XRD) analysis.

Moreover, the coordination modes of amantadine-based Schiff base toward metal ions were also investigated. The importance of α-amylase, α-glucosidase, and alkaline phosphatase in medicinal and biomolecular studies has made it prevalent for scientific studies and commercial applications.[38] Therefore, all the prepared compounds were screened for their ALP, α-amylase, and α-glucosidase inhibition potential.

Results and discussion

Synthesis and characterization of ligand (HL)

Amantadine-based Schiff base ligand (HL) was synthesized as illustrated in Scheme 1. Briefly, 3-allyl-2-hydroxybenzaldehyde was refluxed with amantadine in ethanol in a 1 : 1 molar ratio, while metal complexes were synthesized by refluxing ligand with their corresponding metal salts in a 2 : 1 the molar ratio under reflux conditions.

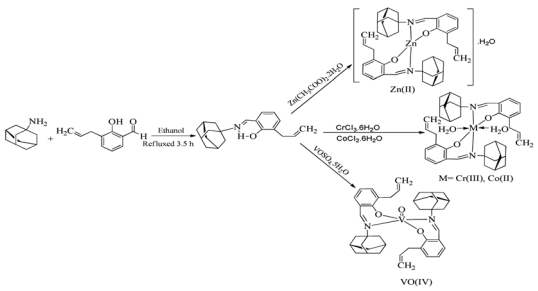

Scheme 1 Synthesis of Schiff base (HL) and its metal complexes a–d; (i) EtOH, refluxed 3.5 h at 90–100 °C; (ii) EtOH, NaOH (0.1%), $Zn(CH_3COO)_2 \cdot 2H_2O$, reflux; EtOH, NaOH (0.1%), $CoCl_2 \cdot 6H_2O$, reflux; EtOH, NaOH (0.1%), $CrCl_3 \cdot 6H_2O$, reflux; EtOH, NaOH (0.1%), $VOSO_4 \cdot 5H_2O$, reflux.

UV-Vis spectra

The UV-Vis spectra of ligand (HL) and its complexes were recorded from 200 to 800 nm at 25 °C in DMSO, as shown in Fig. 1. The ligand showed an absorption band around 323 nm assigned to n → π* transitions.[39] The absorption band of ligand (HL) around 419 nm was assigned to n → π* transition due to intra-ligand charge transfer due to the presence of conjugation in the ligand. The zinc complex exhibited bands around 305 and 375 nm. A band around 305 nm may be due to the –C=N moiety assigned to n → π* transition, while a band around 374 nm may be assigned to LMCT or MLCT. A band that corresponded to the imine function showed a small shift to a shorter wavelength on complexation, indicating ligand coordination to metal through the imine group.[40] At the same time, the cobalt complex exhibited two bands around 365 and 532 nm, which may be due to the –C=N group and d–d transition.[41] Chromium complex exhibited three bands around 356, 405 and 523 nm, which may be assigned to the –C=N group, charge transfer (LMCT or MLCT) and d–d transition. The band corresponding to the –C=N group in the spectrum of ligand showed a slight shift to a longer wavelength on complexation, indicating coordination of ligand to metal through the –C=N group. Similarly, the vanadium complex showed three bands around 347, 450, and 604 nm, which are assigned to the azomethine (–C=N) group, charge transfer (CT), and d–d transitions, respectively.[42]

FT-IR spectra

The observed FT-IR stretching frequencies of the ligand (HL) and its metal compounds are given in Table 1, while the spectra are given in Fig. S1–S5.† The FT-IR spectrum of the Schiff base showed O–H (H-bonded, weak) stretching frequency at 3317 cm^{-1}. Free –OH stretching vibration is commonly observed at 3500–3600 cm^{-1}; lower OH stretching frequency was found due to intramolecular hydrogen bonding.[43] The disappearance of the –OH peak in all the metal complexes indicated the involvement of the –OH group in the complexation.[44] This was also supported by the shifting of C–N stretching frequency from ~1228 cm^{-1} (HL) to the lower wavenumber of 1076 to 1207 cm^{-1} on complexation. Two sharp bands at 2908 cm^{-1} and 2848 cm^{-1}

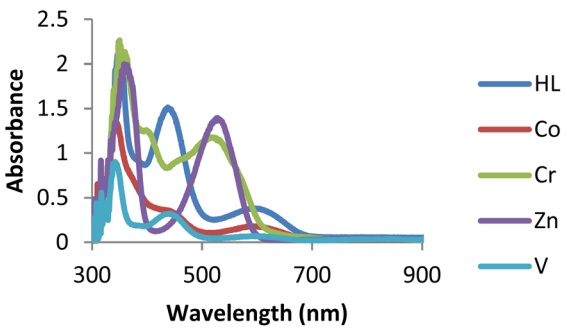

Fig. 1 UV-Vis spectra of ligand and its complexes.

Table 1 Characteristic observed IR spectral bands of novel Schiff base ligand and its metal complexes (cm^{-1})

Compounds	ν(HC=N)	ν(C–N)	ν(M–N)	ν(M–O)	ν(H_2O)	ν(OH)	ν(V=O)
HL	1618	1228	—	—	—	3317	—
Zn(II)	1606	1205	557	480	3464	3296	—
Cr(III)	1608	1076	538	460	3471	3302	
Co(II)	1597	1207	555	445	3464	3286	—
VO(IV)	1622	1118	617	466	—	3383	941

in the FT-IR spectrum of ligand (HL) were assigned to CH_2 antisymmetric and CH_2 symmetric stretching, respectively.[45]

A band observed at 1618 cm^{-1} was assigned to the C=N (azomethine) group in the HL. Increase or decrease in stretching frequencies was observed for the C=N (azomethine) group to the extent 4–25 cm^{-1} on complexations, indicating the involvement of the azomethine (C=N) group in coordination with metal ions.[46] The bands that appeared in the range of 617 to 538 cm^{-1} and 445 to 480 cm^{-1} were due to the metal–nitrogen (M–N) and metal–oxygen (M–O) bond stretching vibrations, respectively. In the case of the vanadium complex, a characteristic sharp band that appeared at 941 cm^{-1} was observed due to V=O vibrations.[47] In the cobalt complex, having a band around 3450 cm^{-1} was assigned to the coordinated water molecules.

Mass spectra

The LC-MS spectrum of HL is given in Fig. S6,† which shows two fragments. The spectrum showed the molecular ion peak at m/z = 296.20, while the second fragmented ion appeared at 152 m/z. The molecular ion peak appeared as a base peak, and the intensity of appeared peaks showed the stability and abundance of fragmented ions.

NMR spectra

^{1}H-NMR spectrum of (*E*)-2-((adamantan-1-ylimino) methyl)-6-allylphenol was recorded in DMSO-d_6 as a solvent (Fig. S7†). A single peak at 14.83 ppm for ligand was assigned to the phenolic hydroxyl proton. Another peak at 8.55 ppm can be attributed to HC=N proton.[48] The CH and CH_2 group from amantadine were identified in the range of 1.70–2.08 ppm. CH_2-methylene peak appeared at 4.99 ppm as doubled. Two H-1-ethylene peaks appeared at 5.02 ppm and 5.07 ppm as triplets, while one H-1-ethylene peak appeared as a multiplet at 5.93 ppm. One triplet peak at 6.79 ppm can be assigned to CH-benzylidenimin, while two CH-benzylidenimin peaks appeared as a doublet at 7.12 and 7.33 ppm.

The ^{13}C-NMR of (*E*)-2-((adamantan-1-ylimino)methyl)-6-allylphenol was recorded in DMSO-d_6 is given in Fig S8.† The obtained chemical shift values corresponding to the carbon atoms were compared with the proposed structure. The carbon atoms present in adamantine showed peaks at 29.24, 36.13, and 42.95 ppm. While the carbon of adamantine directly attached to the nitrogen atom of the –N=C– bond showed a peak at 56.96 ppm. The imine group carbon showed a peak at 161.53 ppm.[49] The carbon atom attached to the hydroxyl group showed a peak at 160.32 ppm. The aromatic carbons in the benzene ring showed peaks at 130.56, 127.91, 116.09, and 132.68 ppm. Aliphatic carbon showed a peak at 33.48 ppm, while two ethylene carbon peaks appeared at 137.15 and 117.76 ppm.

Single crystal XRD analysis for Schiff base (HL) and zinc complex

The single crystals of HL and Zn(II) complex were grown in ethanol; yellow crystals of HL, and colorless crystals of the Zn(II) complex were analyzed using SC-XRD analysis. The crystals were mounted on a goniometer head using grease, shown in Fig. S8.† The data sets were collected on Bruker D8 Venture with PHOTON II detector and Mo microfocus source (Bruker 2016) (λ = 0.71073 Å) (Bruker 2016) under cryo conditions under Oxford Cobra Cryodevice using omega and phi scan methods. The diffracted intensities were processed using APEX3 tools (Bruker, 2016). Analytical absorption correction was applied. Table S1† summarizes the crystallographic and refinement details.

The crystal structures of HL were solved in the monoclinic *Pc* space group, whereas the structure of the Zn complex was solved in the monoclinic $P2_1/c$ space group using Olex2 (Dolomanov) (Fig. 2). Most hydrogen atoms could be located in different Fourier maps; however, they were fixed using a riding model. The bond angles, bond lengths and torsion angles of the ligand and zinc complex are shown in Tables S2 and S3.† In the formation of the zinc complex, the ligand (HL) was deprotonated (L^{-1}) by losing its phenolic proton and behaves as a monobasic. Each ligand acts as a bidentate and is coordinated to the metal ion using its phenolic oxygen and azomethine nitrogen atoms. The zinc complex is tetra-coordinated using a ONON set of donor sites from two ligands to make a distorted tetrahedral geometry, as evidenced by the bond angles around the zinc center, which deviate from the ideal angle of 109° (Table S3†). In the asymmetric unit of the zinc complex, there is one zinc-containing molecule (C1–C40/N1/N2/O1/O2/Zn1) and one water molecule. The bidentate ligand forms two chelating rings (C28/C29/C30/N1/O2/Zn1) and (C8/C9/C10/N1/O2/Zn1). The coordination sphere around the central Zn-atom is composed of phenolic O-atoms (O1 and O2) and imine N-atoms (N1 and N2) from the bidentate chelating ligands. The Zn–O1 and Zn1–O2 bonds are shorter than the Zn1–N1 and Zn1–N2 bonds.

Molar conductivity

The molar conductivity of the synthesized metal complexes was measured in DMSO as solvent at a concentration of 1×10^{-3} moles per dm^3. The conductivity of prepared metal complexes

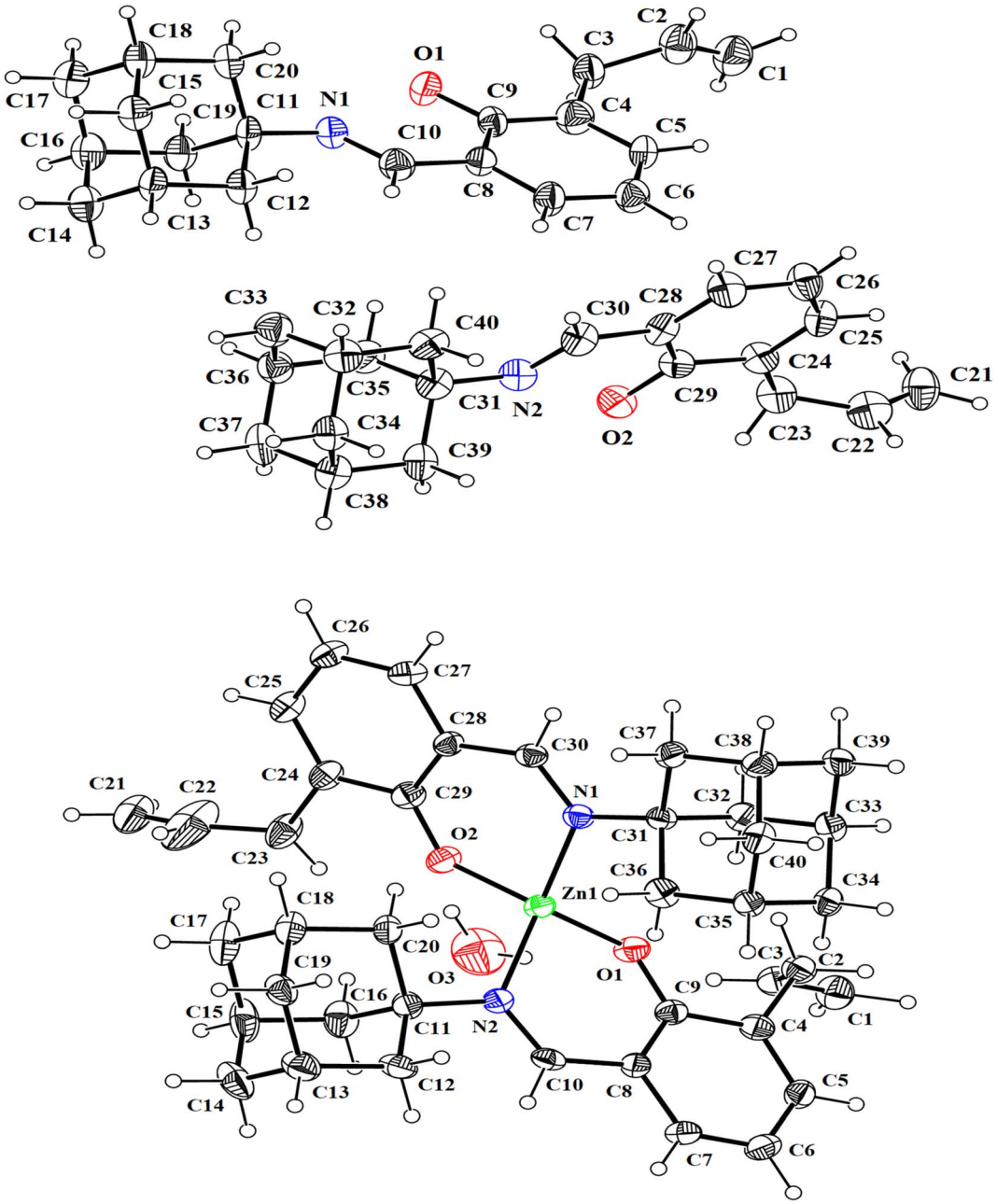

Fig. 2 Thermal ellipsoid plots (@50% probability) for HL and Zn complex show the atom numbering scheme for both models. The figures are drawn using Mercury.[51]

was found to be in the range of 2–12 ohm^{-1} cm^2 mol^{-1}, indicating that all synthesized complexes were non-electrolytes.[50]

Thermal behaviour

The thermogravimetric analysis (TGA) of Schiff base (HL) and its metal complexes was carried out under a nitrogen atmosphere at a heating rate of 10 °C per minute. The thermogram of HL and its complexes are given in Fig. 3 and S10–S13.† The decomposition of synthesized ligand occurred completely in the temperature range of 225–265 °C. The thermal decomposition of prepared metal complexes proceeded in a multi-step process.

The first thermal decomposition step corresponded to the loss of lattice/coordinated water molecules that occurred in the temperature ranges of 84–192 °C, 80–105 °C, and 169–207 °C for cobalt, zinc, and chromium complexes, respectively. Loss of lattice water occurred at a lower temperature between 60–100 °C, while loss of coordinated water molecules occurred above 150 °C.[52] In the case of oxovanadium, the first decomposition occurred around 212–225 °C due to the ligand moieties being lost. The thermogram of the chromium complex indicated the removal of two coordinated water molecules and the substitution of ligands.

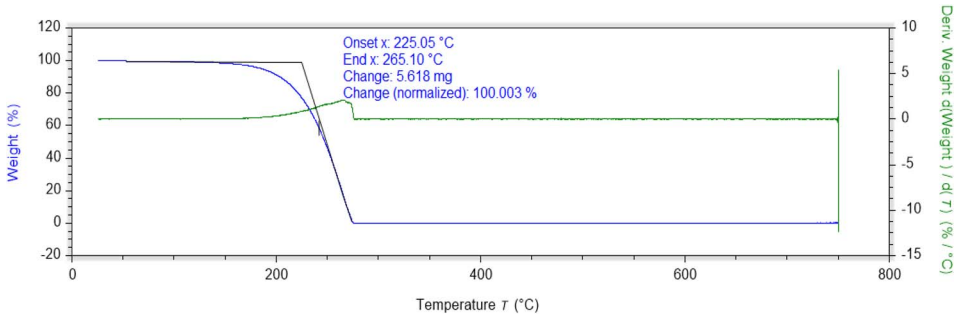

Fig. 3 Thermogram of (*E*)-2-((adamantan-1-ylimino)methyl)-6-allylphenol (HL).

The second decomposition occurred in the temperature ranges of 335–370 °C, 333–385 °C, 446–455 °C, and 660–708 °C for zinc, cobalt, chromium, and vanadium complexes, respectively, indicating the loss of ligand moieties. The third decomposition step occurred in the temperature ranges of 449–513 °C, 450–491 °C, and 880–918 °C, indicating the loss of the remaining ligand for zinc, cobalt, and chromium complexes, respectively. In the case of zinc and cobalt complexes, the last decomposition suggested the formation of metal oxide. In the case of chromium and vanadium complexes, decomposition did not complete even at 900 °C, leaving behind undecomposed material; therefore, the last decomposition residue was not possible to calculate. The synthesized metal complexes were found to be highly thermally stable as compared to the ligand (HL).

ALP enzyme inhibition studies

The alkaline phosphate activity takes advantage of the fact that the ALP enzyme is non-specific and utilizes the substrate *para*-nitrophenyl phosphate (*p*-NPP) to give a yellow-colored *p*-nitrophenolate ion, which is used to monitor the reaction.[53] The inhibitory effect of various synthesized compounds on the alkaline phosphatase enzyme activity was studied. Ligand (HL) failed to show activity against ALP. Among all metal complexes, the vanadium complex showed a remarkable inhibition effect. The ALPs inhibition was attributed to vanadium coordination with the enzyme, making the enzyme's active sites unavailable for the substrate by replacing calcium and zinc from the enzyme.

The second possibility is that the enzyme binds with vanadium more effectively than the substrate. The exact inhibition mechanism of ALP activity is still unknown.[54] Zinc complex also inhibited the enzyme in a concentration-dependent manner by inactivating the enzyme, as confirmed by the decrease in the production of *p*-nitrophenolate ions and hence less absorbance was recorded at 405 nm.[55] Cobalt complex showed less

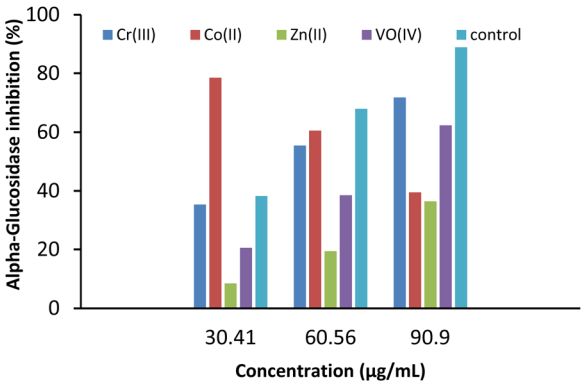

Fig. 5 Concentration-dependent inhibition of α-glucosidase by the synthesized compounds. Mean inhibition (%) ± SD^n significantly different ($p < 0.05$), n = values are given as the mean of three replicates.

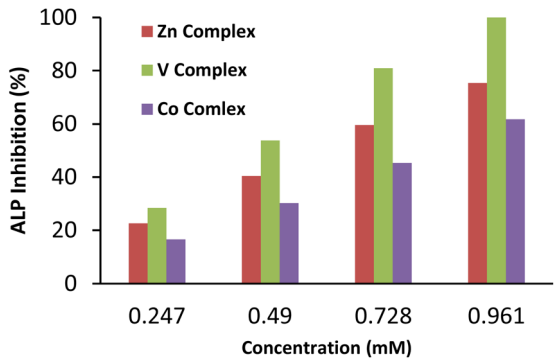

Fig. 4 Concentration-dependent inhibition of ALP by synthesized compounds. Mean inhibition (%) ± SD^n significantly different ($p < 0.05$), n = values are given as the mean of three replicates.

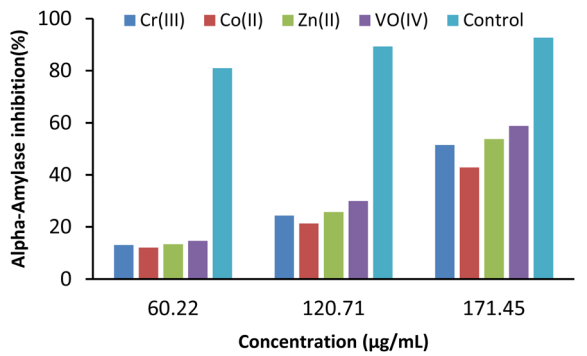

Fig. 6 Concentration-dependent inhibition of α-amylase by synthesized compounds. Mean inhibition (%) ± SD^n significantly different ($p < 0.05$), n = values are given as the mean of three replicates.

Table 2 *In vitro* alpha-amylase and alpha-glucosidase inhibitory studies of synthesized complexes. Mean inhibition (%) ± SD^n significantly different ($p < 0.05$), n = values are given as the mean of three replicates

	IC_{50} (μg mL^{-1})	
Compounds	α-Glucosidase	α-Amylase
Zn(II)	169.39 ± 2.63	108.51 ± 0.89
Co(II)	89.84 ± 1.06	157.81 ± 1.99
Cr(iii)	104.25 ± 1.78	116.16 ± 1.6
VO(iv)	122.38 ± 0.9	97.47 ± 0.9
Control	84.15 ± 1.20	78.57 ± 0.99

inhibition than vanadium and zinc complexes against ALP.[56] The inhibition studies revealed the concentration-dependent enzyme inhibition effect. An increase in the concentration of metal complexes decreases the activity of the ALP (Fig. 4).

Anti-diabetic activity

α-Glucosidase and α-amylase inhibition studies. α-Glucosidase inhibitory activities were performed at 30.41, 60.56, and 90.90 μg mL^{-1}, while α-amylase inhibition studies were carried out at 60.22, 120.71, and 171.45 μg mL^{-1}. The results are shown in Fig. 5 and 6. Both inhibitory activities were increased with the

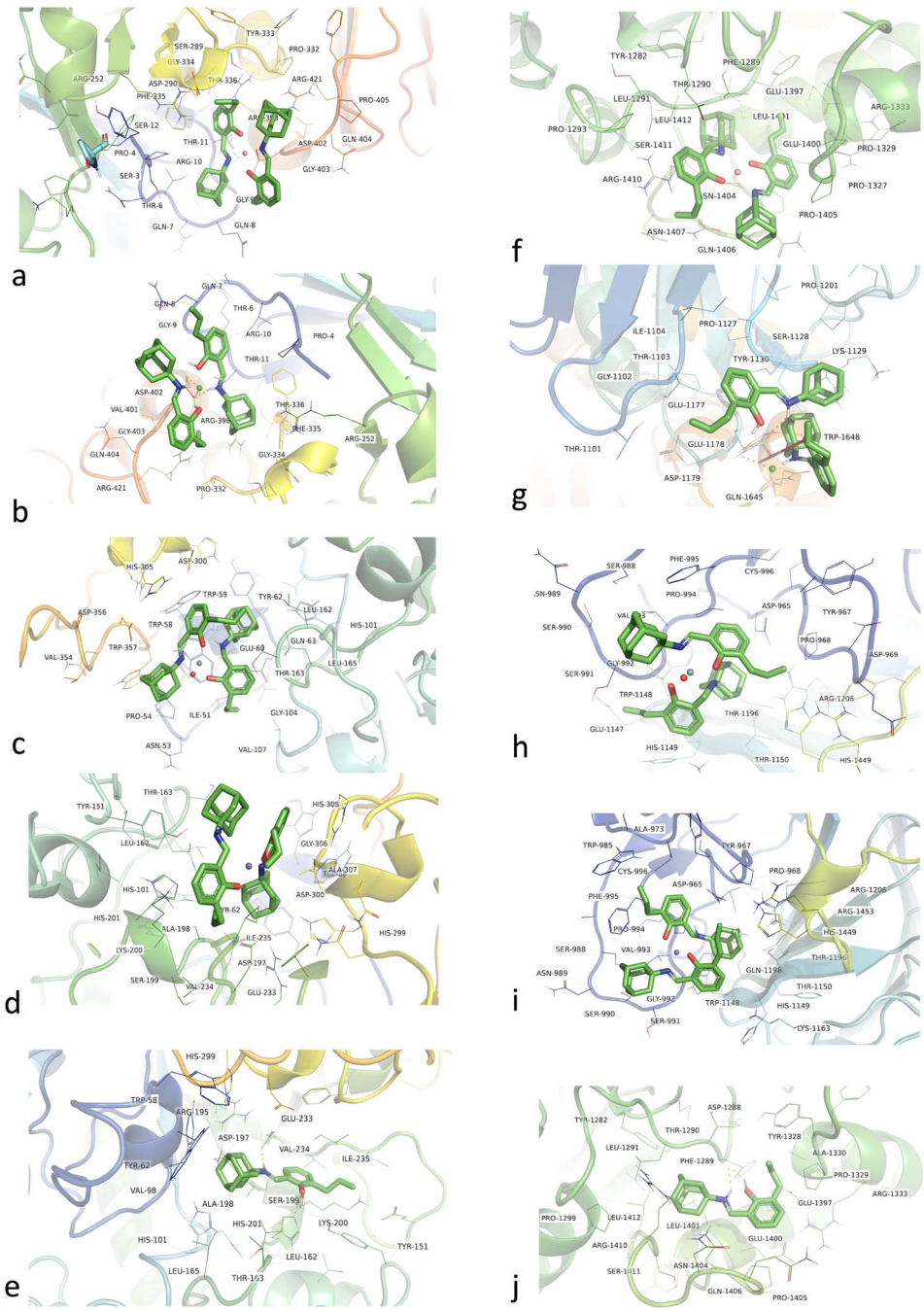

Fig. 7 Anti α-amylase activity (a–e) and anti α-glucosidase activity (f–j) of the ligand and metal complexes.

concentration of inhibitors, which illustrated a strong dose-dependent response. The screening against α-glucosidase enzyme demonstrated that Co(II) exhibited the highest inhibitory action with an IC_{50} value of 89.84 ± 1.06 μg mL^{-1}, followed by Cr(III), VO(IV) and Zn(II) with IC_{50} values of 104.25 ± 1.78, 122 ± 0.9, and 169 ± 2.6 μg mL^{-1}, respectively, while VO(IV) complex displayed the highest α-amylase inhibitory capacity with an IC_{50} value of 97.47 ± 0.9 μg mL^{-1} followed by Zn(II), Cr(III), and Co(II) with IC_{50} values of 108.51 ± 0.89, 116 ± 1.67, and 157.81 ± 1.99 μg mL^{-1}, respectively as shown in Table 2.

***In silico* antidiabetic studies.** The ligand and metal complexes were virtually screened against the α-amylase (PDB ID 4W93) and α-glucosidase (PDB ID 3TOP) structures from the human. In the case of α-amylase, HL and its complexes shared the same binding pocket consisting of TRP58, TYR62, VAL98, HIS101, TYR151, LEU162, THR163, LEU165, ARG195, ASP197, ALA198, SER199, LYS200, HIS201, GLU233, VAL234, ILE235, HIS 299, ASP300, HIS305, GLY306, and ALA307 residues (Fig. 7a–e). VO(IV), Zn(II), and Cr(III) complexes have shown better binding to α-amylase in comparison to ligand with the binding energies of −12.50, −10.38, and 10.75 kcal mol^{-1} and dissociation constants of 130, 200, and 840 nM, respectively. HL and Co(II) complex have shown comparable binding energies (−9.18 and −9.13 kcal mol^{-1}) and dissociation constants (190 and 200 nM).

In the case of α-glucosidase, HL was found to bind in a different binding pocket than the metal complexes. This site was consisted of residues including TYR1282, ASP1288, PHE1289, THR1290, LEU1291, PRO1299, TYR1328, PRO1329, ALA1330, ARG1333, GLU1397, GLU1400, LEU1401, ASN1404, PRO1405, GLN1406, ARG1410, SER1411, and LEU1412 (Fig. 7f–j). All metal complexes shared the same binding site consisting of ASP965, TYR967, PRO968, ALA973, TRP985, SER988, ASN989, SER990, SER991, GLY992, VAL993, PRO994, PHE995, CYS996, TRP1148, HIS1149, THR1150, LYS1163, THR1196, GLN1198, ARG1206, HIS1449, and ARG1453 residues. Here, Co(II) and VO(IV) complexes exhibited the best binding energies, *i.e.*, −10.90 and −10.53 kcal mol^{-1}, and dissociation constants, *i.e.*, 10.88 and 18.96 nM. HL showed binding energy of 10.59 kcal mol^{-1} and a dissociation constant of 12.24 nM. Overall, all metal complexes and ligands have shown promising antidiabetic potential in terms of α-amylase (PDB ID 4W93) and α-glucosidase inhibition.

Experimental

All the used organic solvents and metal salts were of analytical grade, purchased from Sigma Aldrich, and used without purification except where mentioned. IR Prestige-21 (Shimadzu) was used to record FT-IR spectra. UV-Vis spectra were recorded on a Shimadzu UV 240 spectrophotometer. The Elico-CM82 Conductivity Bridge was used to measure molar conductance at room temperature. Silica gel (60 F254Merk) coated Al sheets were used for thin-layer chromatography. In both positive and negative ion ESI modes, a mass spectrum was recorded on an Agilent 6224 Time of Flight (TOF) LC-MS mass spectrometer. NMR (^1H and ^{13}C) spectra were recorded on a Bruker US400 spectrometer at 400 and 100 MHz in DMSO-d_6. An Exeter Analytical Inc-CE-440 Elemental Analyzer was used to carry out elemental analysis of the prepared compounds. The melting points of the products were determined by using the Gallenkamp digital melting point apparatus (MFB-595-010M). APEX3 (Bruker, 2016), SAINT (Bruker, 2016) and Mercury 4.0 were used from visualization to analysis, design and prediction. A thermogravimetric analyzer (TGA Q500) was used to study the thermal degradation trend of compounds at a heating rate of 10 °C min^{-1} under a nitrogen atmosphere with a flow rate of 5 mL min^{-1}. Alkaline phosphatase inhibitory activity was screened by following the reported method.

Synthesis of (*E*)-2-((adamantan-1-ylimino)methyl)-6-allylphenol (HL)

Amantadine-based Schiff base ligand and its complexes were synthesized using the literature method with a few modifications (Scheme 1).[57] An ethanolic solution (25 mL) of 3-allyl-2-hydroxybenzaldehyde (1.07 g, 6.6 mmol) was prepared in a 100 mL round bottom flask. Amantadine (1 g, 6.6 mmol) was dissolved in ethanol (15 mL) and added to the above solution dropwise, and then the whole mixture was refluxed for 3.5 hours. The progress of the reactions was monitored by thin-layer chromatography. After the completion of the reaction, the resulting solution was concentrated to half of its original volume by evaporation and left for two days to get a yellow oily product, which was further converted into yellow crystals by the addition of cold ethanol. These bright yellow crystals were vacuum filtered, washed thrice with ice-cold ethanol, recrystallized from ethanol, and dried in the desiccator. Color: yellow; yield: 80%; melting point: 85 °C; UV/Vis: 271, 326, 420; ESI-MS: 296.20$[M + H]^+$; FT-IR: (KBr disc) ν/cm^{-1}: 1618 (HC=N), 1547 (C=C), 1228 (C–N), 2908, 2848 (C–H-aromatic, str), 3317 (OH-aromatic), 3062 (vinyl CH_2, str); ^1H-NMR (400 MHz, DMSO-d_6) δ ppm; 1.70 (m, CH_2, 1-adamantane), 1.87 (d, CH_2, 1-adamantane), 2.08 (m, CH_2, 1-adamantane), 4.99 (d, CH_2, methylene), 5.02 (t, H, 1-ethylene), 5.07 (t, H, 1-ethylene), 5.93 (m, H, 1-ethylene), 14.83 (s, OH-alcohol), 6.79 (t, CH-benzylidenimin), 7.12 (d, CH-benzylidenimin), 7.33 (d, CH-benzylidenimin), 8.55 (s, CH=N) ^{13}C-NMR (DMSO-d_6) δ ppm; 29.24 (C1), 33.48 (C2), 36.13 (C3), 42.95 (C4), 56.96 (C5), 116.09 (C6), 117.76 (C7), 127.91 (C8), 130.56 (C9), 132.68 (C10), 137.15 (C11), 160.32 (C12), 161.53 (C13). CHN analysis: chemical formula: $C_{20}H_{25}NO$ (exact mass: 295.19): calcd: C, 81.31; H, 8.53; N, 4.74. Found: C, 81.89; H, 8.09; N, 4.99.

Synthesis of metal complexes from Schiff base ligand (HL)

Complexes were prepared by the same general procedure. To the hot ethanolic solution (15 mL) of HL (2 mmol), a hot ethanolic (15 mL) solution of corresponding metal salt like $Zn(CH_3COO)_2 \cdot 2H_2O$, $CoCl_2 \cdot 6H_2O$, $CrCI_3 \cdot 6H_2O$, or $VOSO_4 \cdot 5H_2O$ (1 mmol) was added drop by drop with stirring constantly and pH of the reaction mixture was adjusted to 8–8.5 using an ethanolic solution of NaOH (0.1%) and then refluxed at 90–100 °C for 3–4 h. The resulting mixture was cooled and left overnight at room temperature to get colored solid products,

which were filtered out, washed with ice-cold ethanol, recrystallized with appropriate solvents and dried in a desiccator.

Synthesis of zinc complex

Color: colorless crystals; yield: 56%; melting point: 145 °C; UV/Vis: 365, 532; molar conductance (Ω^{-1} cm^2 mol^{-1}) 2; FT-IR: (KBr disc) ν/cm^{-1}: 1606 (HC═N), 1546 (C═C), 1205 (C–N), 2912, 2852 (C–H-aromatic, str), 3464 (H_2O), 557 (Zn–N), 480 (Zn–O). CHN analysis: chemical formula: $C_{40}H_{48}N_2O_2Zn$ (exact mass: 654.20): calcd: C, 73.44; H, 7.40; N, 4.28; Found: C, 73.56; H, 7.69; N, 4.58.

Synthesis of chromium complex

Color: green; melting point: 180 °C; yield: 43%; UV/Vis: 356, 405, 523; molar conductance (Ω^{-1} cm^2 mol^{-1}): 9; FT-IR: (KBr disc) ν/cm^{-1}: 1608 (HC═N), 1442 (C═C), 1076(C–N), 2906 (C–H-aromatic, str), 538(Cr–N), 460 (Cr–O), 3471(coordinated water). CHN analysis: chemical formula: $C_{40}H_{52}N_2O_4Cr$ (exact mass: 672): calcd: C, 77.06; H, 7.76; N, 4.49; found: C, 77.99; H, 7.81; N, 4.48.

Synthesis of cobalt complex

Color: orange; yield: 57%; melting point: 170 °C; UV/Vis: 265, 374; molar conductance (Ω^{-1} cm^2 mol^{-1}): 3.5; FT-IR: (KBr disc) ν/cm^{-1}: 1597 (HC═N), 1544.9 (C═C), 1207(C–N), 2910, 2850 (C–H-aromatic, str), 555 (Co–N), 445 (Co–O), 3464 (water peak). CHN analysis: chemical formula: $C_{40}H_{52}N_2O_4Co$ (exact mass: 683.30): calcd: C, 74.17; H, 7.47; N, 4.32; found; C, 74.28; H, 7.53; N, 4.65.

Synthesis of oxovanadium complex

Color: dark green; mp: above 300 °C; yield: 60%; UV/Vis: 347, 450, 604; molar conductance (Ω^{-1} cm^2 mol^{-1}):12; FT-IR: (KBr disc) ν/cm^{-1}: 1622 (HC═N), 1446 (C═C), 1118.7 (C–N), 2904, 2848 (C–H-aromatic, str), 941 (V═O), 543 (V–N). CHN analysis: chemical formula: $C_{40}H_{48}N_2O_3V$ (exact mass: 655.31): calcd: C, 73.26; H, 7.38; N, 4.27; found; C, 73.16; H, 7.48; N, 4.57.

Assay of alkaline phosphatase activity

An assay for the inhibitory effects of metal complexes on alkaline phosphatase enzyme (ALP) was performed following the reported methodology.[58] To prepare the working substrate, reagent A (diethanolamine having pH 9.8, mol dm^{-3} and $MgCI_2$ 0.5 mmol dm^{-3}) and reagent B (*p*-nitrophenyl phosphate 50 mmol dm^{-3}) were prepared. The prepared substrate was incubated at 25 °C for 5 minutes. 40 μL of human serum-containing ALP with an activity of 165 IU L^{-1} was taken in a cuvette, and 2 mL of the prepared substrate was added to it and incubated for 1 min. After that, absorbance was measured to confirm the enzymatic activity, which was used as a blank. ALP on hydrolysis of *p*-NPP under basic conditions yielded *p*-nitrophenol, which produced a *p*-nitrophenolate ion of yellow-colored and absorbance was measured at 405 nm. To study the inhibition effect of synthesized compounds, the concentration of ALP and prepared substrate was kept constant, but the quantities of inhibitors, HL, and its metal complexes were increased periodically (10, 20, 30, and 40 μL) in each absorbance measurement from 12.5 mM stock solution. Before absorbance measurements, each sample was incubated for 3 min, and after every min for at least 5 min, the decrease in absorbance was observed. To calculate the percentage inhibition, an average value of the measured absorbance was taken. All ALP studies were made in triplicate. The activity of the Cr(III) complex was not recorded due to its toxicity.

α-Amylase inhibition assay. α-Amylase inhibition assay was performed *in vitro* using the reported iodine starch method by amending slightly.[59] To prepare the reaction mixture, 10 μL of α-amylase (0.1 mg mL^{-1}) was dissolved in 10 mM phosphate buffer (pH 6.9, NaCl 6 mM) and mixed with varying concentrations of ligand and its metal complexes. The reaction mixture was then incubated for 30 min at 37 °C. After incubation, 40 μL of 1% starch solution was poured into it and incubated for 10 min at 37 °C. The reaction was terminated by adding 20 μL of 1 M HCl to the reaction mixture, and 75 μL of iodine solution was added afterwards. The quantification of the color imparted to the reaction mixture by iodine solution (as the yellow color of iodine changes to deep blue color if starch is present) was done electrometrically at 580 nm wavelength. Acarbose (50 μg mL^{-1}) was used as a positive control. Percentage inhibition of activity was calculated from the following equation.

$$\%\ \text{Inhibition activity} = [A_{\text{sample}} - A_{\text{blank}}/A_{\text{control}} - A_{\text{blank}}] \times 100$$

Here, A = absorbance. The concentration of used inhibitors required for inhibiting 50% of α-amylase inhibition studies under the assay environment was defined as the IC_{50} value. The data presented are mean ± SD obtained from 96-well-plate readers for all *in vitro* experiments.

α-Glucosidase inhibition assay. The α-glucosidase inhibitory activity was measured following a reported method with slight modifications.[60,61] Briefly, 10 μL of sample solution and 30 μL of 0.1 M phosphate buffer (pH 6.8) containing α-glucosidase solution (0.2 U mL^{-1}) was incubated in 96 well plates at 37 °C for 10 min. After pre-incubation, 30 μL of 5 mM *p*-nitrophenyl-α-D-glucopyranoside (PNPG) solution in 0.1 M phosphate buffer (pH 6.8) was added to each well incubated at 37 °C for another 20 min. Then the reaction was stopped by adding 40 μL of 0.2 M Na_2CO_3 into each well, and absorbance readings (A) were recorded at 405 nm by a microplate reader (SpectraMax®, M2/M2^e, Molecular device Co., Sunnyvale, CA, USA) and compared to a control. Acarbose (50 μg mL^{-1}) was used as a positive control. Different concentrations of test samples were used. The α-glucosidase inhibitory activity was expressed as inhibition% and was calculated as follows:

$$\text{Inhibition}\ (\%) = (A_{\text{control}} - A_{\text{sample}})/A_{\text{control}} \times 100$$

The concentration of inhibitors required for inhibiting 50% of the α-glucosidase activity under the assay conditions was defined as the IC_{50} value. The concentration of used inhibitors required for inhibiting 50% of α-amylase inhibition studies under the assay environment was defined as the IC_{50} value. The

data presented are means ± SD obtained from 96-well-plate readers for all *in vitro* experiments.

In silico antidiabetic studies

To elucidate the mode of inhibition of ligand (HL) and its metal complexes with α-amylase and α-glucosidase *in silico* studies were employed. The structures of the HL and its complexes were optimized using Avogadro and YASARA software 20.7.4. The protein three-dimensional crystal structures of α-amylase and α-glucosidase were obtained from Protein Data Bank (PDB) as PDB IDs 4W93 and 3TOP, respectively. A modified Autodock-LGA algorithm employed in YASARA software[62] was used to map the protein–ligand interactions using the previously described method.[63,64] Visualization was obtained by LigPlus[65] and PyMol.

Statistical analysis

Analysis was carried out at every time point for each experiment in triplicates. The results were analyzed statistically by ANOVA. Statistical significance was accepted at a level of $p < 0.05$.

Conclusion

Herein, the synthesis of amantadine-based Schiff base and its metal complexes has been reported. The synthesized compounds were successfully characterized by different analytical techniques. The molecular geometries of ligand and zinc complex were determined by single crystal X-ray crystallography. The zinc complex showed a distorted tetrahedral geometry. To investigate the bio profile of the synthesized compounds, alkaline phosphatase inhibition and antidiabetic activities were performed. All of the synthesized compounds except ligand were found effective for alkaline phosphatase inhibition. The Co(II) and Cr(III) complexes were found potent inhibitors of α-glucosidase while in the case of α-amylase studies, Zn(II) and VO(IV) complexes were found potent inhibitors. Molar conductance determined the non-electrolytic nature of complexes while thermal analysis confirmed the high thermal stability of complexes as compared to ligand –HL.

Author contributions

Conceptualization, Aliya Ajaz and Muhammad Ashraf Shaheen; methodology, Muhammad Ashraf Shaheen, Aliya Ajaz, Abu Bakar Siddique; software, Maqsood Ahmed; data collection, structure solution, refinement, validation, Khurram Shahzad Munawar, Muhammad Fayyaz ur Reman and Abdul Karim; formal analysis, Nazir Ahmad; investigation, Abdul Karim; resources, Muhammad Ashraf Shaheen; data curation, Aliya Ajaz; writing—original draft preparation, Aliya Ajaz; writing—review and editing, Abu Bakar Siddique; visualization, Muhammad Fayyaz ur Reman; supervision, Muhammad Ashraf Shaheen; project administration, Muhammad Ashraf Shaheen. All authors have read and agreed to the published version of the manuscript.

Conflicts of interest

There are no conflicts to declare.

References

1 H. Kargar, M. Nateghi-Jahromi, M. Fallah-Mehrjardi, R. Behjatmanesh-Ardakani, K. S. Munawar, S. Ali, M. Ashfaq and M. N. Tahir, Synthesis, spectral characterization, crystal structure and catalytic activity of a novel dioxomolybdenum Schiff base complex containing 4-aminobenzhydrazone ligand: a combined experimental and theoretical study, *J. Mol. Struct.*, 2022, **249**, 131645.
2 A. Sharma and M. Shah, Synthesis and characterization of some transition metal complexes derived from bidentate Schiff base ligand, *J. Appl. Chem.*, 2013, **3**, 62–66.
3 H. Yu, W. Zhang, Q. Yu, F.-P. Huang, H.-D. Bian and H. Liang, Ni(II) complexes with Schiff base ligands: preparation, characterization, DNA/protein interaction and cytotoxicity studies, *Molecules*, 2017, **22**, 1772.
4 G. G. Mohamed, E. M. Zayed and A. M. Hindy, Coordination behaviour of new bis Schiff base ligand derived from 2-furan carboxaldehyde and propane-1,3-diamine. Spectroscopic, thermal, anticancer and antibacterial activity studies, *Spectrochim. Acta, Part A*, 2015, **145**, 76–84.
5 K. T. Tadele, Antioxidant activity of Schiff bases and their metal complexes: a recent review, *J. Pharm. Med. Res.*, 2017, **3**, 73–77.
6 A. N. Srivastva, N. P. Singh and C. K. Shriwastaw, *In vitro* antibacterial and antifungal activities of binuclear transition metal complexes of ONNO Schiff base and 5-methyl-2,6-pyrimidine-dione and their spectroscopic validation, *Arabian J. Chem.*, 2016, **9**, 48–61.
7 M. M. Abd-Elzaher, A. A. Labib, H. A. Mousa, S. A. Moustafa, M. M. Ali and A. A. El-Rashedy, Synthesis, anticancer activity and molecular docking study of Schiff base complexes containing thiazole moiety, *Beni-Suef Univ. J. Basic Appl. Sci.*, 2016, **5**, 85–96.
8 E. Król and Z. Krejpcio, Evaluation of anti-diabetic potential of chromium(III) propionate complex in high-fat diet fed and STZ injected rats, *Food Chem. Toxicol.*, 2011, **49**(12), 3217–3223.
9 A. Thakar, K. Joshi, K. Pandya and A. Pancholi, Coordination modes of a Schiff base derived from substituted 2-aminothiazole with chromium(III), manganese(II), iron(II), cobalt(II), nickel(II) and copper(II) metal ions: synthesis, spectroscopic and antimicrobial studies, *Eur. J. Chem.*, 2011, **8**, 282061.
10 S. M. Khalil, M. Shebl and F. S. Al-Gohani, Zinc(II) thiosemicarbazone complex as a ligand towards some transition metal ions: synthesis, spectroscopic and antimicrobial studies, *Acta Chim. Slov.*, 2010, **57**, 716–725.
11 M. Ngugi, J. Njagi, C. Kibiti and M. Mwenda, Pharmacological management of diabetes mellitus, *Asian J. Biochem. Pharm. Res.*, 2012, **2**, 2012.

12 A. Malik, M. H. Mehmood and M. Fayyaz-ur-Rehman, Journey of 100 years of insulin discovery, from past to present: an overview, *Multidiscip. Rev.*, 2021, **1**, 19–34.
13 N. G. E. R. Etsassala, J. A. Badmus, J. L. Marnewick, E. I. Iwuoha, F. Nchu and A. A. Hussein, Alpha-Glucosidase and alpha-amylase inhibitory activities, molecular docking, and antioxidant capacities of salvia aurita constituents, *Antioxidants*, 2020, **9**, 1149.
14 S. S. Nair, V. Kavrekar and A. Mishra, *In vitro* studies on alpha amylase and alpha glucosidase inhibitory activities of selected plant extracts, *Eur. J. Exp. Biol.*, 2013, **3**, 128–132.
15 K. Balan, P. Ratha, G. Prakash, P. Viswanathamurthi, S. Adisakwattana and T. Palvannan, Evaluation of *in vitro* α-amylase and α-glucosidase inhibitory potential of N_2O_2 Schiff base Zn complex, *Arabian J. Chem.*, 2017, **10**, 732–738.
16 K. H. Thompson, J. Chiles, V. G. Yuen, J. Tse, J. H. McNeill and C. Orvig, Comparison of anti-hyperglycemic effect amongst vanadium, molybdenum and other metal maltol complexes, *J. Inorg. Biochem.*, 2004, **98**, 683–690.
17 A. Levina, A. I. McLeod, J. Seuring and P. A. Lay, Reactivity of potential anti-diabetic molybdenum(VI) complexes in biological media: A XANES spectroscopic study, *J. Inorg. Biochem.*, 2007, **101**, 1586–1593.
18 M. A. Mahmoud, S. A. Zaitone, A. M. Ammar and S. A. Sallam, Synthesis, spectral, thermal and insulin-enhancing properties of oxovanadium(IV) complexes of metformin Schiff-bases, *J. Therm. Anal. Calorim.*, 2017, **128**, 957–969.
19 R. Miyazaki, H. Yasui and Y. Yoshikawa, α-Glucosidase inhibition by new Schiff base complexes of Zn(II), *Open J. Inorg. Chem.*, 2016, **6**, 114–124.
20 N. Ali, M. Tahir, M. Iqbal, K. S. Munawar and S. Perveen, Synthesis, characterization, crystal structures, enzyme inhibition, DNA binding, and electrochemical studies of zinc(II) complexes, *J. Coord. Chem.*, 2014, **67**, 1290–1308.
21 A. Rauf, A. Shah, K. S. Munawar, A. A. Khan, R. Abbasi, M. A. Yameen, A. M. Khan, A. R. Khan, I. Z. Qureshi, H.-B. Kraatz and R. Zia ur, Synthesis, spectroscopic characterization, DFT optimization and biological activities of Schiff bases and their metal (II) complexes, *J. Mol. Struct.*, 2017, **1145**, 132–140.
22 J. Szklarzewicz, A. Jurowska, M. Hodorowicz, R. Gryboś, K. Kruczała, M. Głuch-Lutwin and G. Kazek, Vanadium complexes with salicylaldehyde-based Schiff base ligands—structure, properties and biological activity, *J. Coord. Chem.*, 2020, **73**, 986–1008.
23 J. D. Siqueira, A. C. O. Menegatti, H. Terenzi, M. B. Pereira, D. Roman, E. F. Rosso, P. C. Piquini, B. A. Iglesias and D. F. Back, Synthesis, characterization and phosphatase inhibitory activity of dioxidovanadium(V) complexes with Schiff base ligands derived from pyridoxal and resorcinol, *Polyhedron*, 2017, **130**, 184–194.
24 K. O. Ogunniran, K. O. Ajanaku, O. O. James, O. O. Ajani, J. A. Adekoya and O. C. Nwinyi, Synthesis, characterization, antimicrobial activity and toxicology study of some metal complexes of mixed antibiotics, *Afr. J. Pure Appl. Chem.*, 2008, **2**, 69–74.
25 M. R. Malik, V. Vasylyeva, K. Merz, N. Metzler-Nolte, M. Saleem, S. Ali, A. A. Isab, K. S. Munawar and S. Ahmad, Synthesis, crystal structures, antimicrobial properties and enzyme inhibition studies of zinc(II) complexes of thiones, *Inorg. Chim. Acta*, 2011, **376**, 207–211.
26 J. Jimenez, I. Chakraborty, M. Rojas-Andrade and P. K. Mascharak, Silver complexes of ligands derived from adamantylamines: water-soluble silver-donating compounds with antibacterial properties, *J. Inorg. Biochem.*, 2017, **168**, 13–17.
27 J. Staničová, P. Miskovsky and V. Sutiak, Amantadine: an antiviral and antiparkinsonian agent, *Vet. Med.*, 2001, **46**, 244–256.
28 J. Wang, Y. Wu, C. Ma, G. Fiorin, J. Wang, L. H. Pinto, R. A. Lamb, M. L. Klein and W. F. Degrado, Structure and inhibition of the drug-resistant S31N mutant of the M2 ion channel of influenza A virus, *Proc. Natl. Acad. Sci. U. S. A.*, 2013, **110**, 1315–1320.
29 J. Liu, D. Obando, V. Liao, T. Lifa and R. Codd, The many faces of the adamantyl group in drug design, *Eur. J. Med. Chem.*, 2011, **46**, 1949–1963.
30 P. Lorenzo, R. Alvarez, M. A. Ortiz, S. Alvarez, F. J. Piedrafita and Á. R. de Lera, Inhibition of IκB kinase-β and anticancer activities of novel chalcone adamantyl arotinoids, *J. Med. Chem.*, 2008, **51**, 5431–5440.
31 I. A. Shehadi, F. A. Delmani, A. M. Jaber, H. Hammad, M. A. AlDamen, R. A. Al-Qawasmeh and M. A. Khanfar, Synthesis, characterization and biological evaluation of metal adamantyl 2-pyridylhydrazone complexes, *Molecules*, 2020, **25**, 2530.
32 B. M. Liu, P. Ma, X. Wang, Y. M. Kong, L. P. Zhang and B. Liu, Synthesis of three rimantadine Schiff bases and their biological effects on serum albumin, *Iran. J. Pharm. Res.*, 2014, **13**, 1183–1190.
33 D. Armstrong, F. Taullaj, K. Singh, B. Mirabi, A. Lough and U. Fekl, Adamantyl metal complexes: new routes to adamantyl anions and new transmetallations, *Dalton Trans.*, 2017, **46**, 6212–6217.
34 A. Stimac, M. Šekutor, K. Mlinarj -Majerski, L. Frkanec and R. Frkanec, Adamantane in drug delivery systems and surface recognition, *Molecules*, 2017, **22**, 297.
35 A. P. Mishra and M. Soni, Synthesis, structural, and biological studies of some Schiff bases and their metal complexes, *Met.-Based Drugs*, 2008, **2008**, 875410.
36 A. Halámiková, P. Heringová, J. Kaspárková, F. P. Intini, G. Natile, A. Nemirovski, D. Gibson and V. Brabec, Cytotoxicity, mutagenicity, cellular uptake, DNA and glutathione interactions of lipophilic trans-platinum complexes tethered to 1-adamantylamine, *J. Inorg. Biochem.*, 2008, **102**, 1077–1089.
37 A. K. d. S. Pereira, C. M. Manzano, D. H. Nakahata, J. C. T. Clavijo, D. H. Pereira, W. R. Lustri and P. P. Corbi, Synthesis, crystal structures, DFT studies, antibacterial assays and interaction assessments with biomolecules of new platinum(II) complexes with adamantane derivatives, *New J. Chem.*, 2020, **44**, 11546–11556.

38 G. Dong and J. Gregory Zeikus, Purification and characterization of alkaline phosphatase from Thermotoga neapolitana, *Enzyme Microb. Technol.*, 1997, **21**, 335–340.

39 A. Çapan, S. Uruș and M. Sönmez, Ru(III), Cr(III), Fe(III) complexes of Schiff base ligands bearing phenoxy groups: application as catalysts in the synthesis of vitamin K3, *J. Saudi Chem. Soc.*, 2018, **22**, 757–766.

40 F. Nazir, I. F. Bukhari, M. Arif, M. Riaz, S. Naqvi, M. R. Schiff base, T. H. Bokhari and M. A. Jamal, Antibacterial studies and Schiff base metal complexes with some novel antibiotics, *Int. J. Curr. Pharm. Res.*, 2013, **5**, 40–47.

41 A. Arumugam, S. Guhanathan and G. Elango, Co(II), Ni(II) and Cu(II) complexes with Schiff base ligand: synthesis, characterization, antimicrobial studies and molecular docking studies, *SOJ Mater. Sci. Eng.*, 2017, **5**, 1–12.

42 P. U. Gawande, P. R. Mandlik and A. S. Aswar, Synthesis and characterization of Cr(III), Mn(III), Fe(III), VO(IV), Zr(IV) and UO2(VI) complexes of Schiff base derived from isonicotinoyl hydrazine, *Indian J. Pharm. Sci.*, 2015, 376.

43 A. Bartyzel, Synthesis, thermal study and some properties of N_2-O_2-donor Schiff base and its Mn(III), Co(II), Ni(II), Cu(II) and Zn(II) complexes, *J. Therm. Anal. Calorim.*, 2017, **127**, 2133–2147.

44 W. A. Mahmoud, Z. M. Hassan and R. w. Ali, Synthesis and spectral analysis of some metal complexes with mixed Schiff base ligands 1-[2-(2-hydroxybenzylideneamino)ethyl] pyrrolidine-2,5-dione(HL1) and (2-hydroxybenzylidene) glycine (HL2), *J. Phys.: Conf. Ser.*, 2020, **1660**, 012027.

45 M. Arayne, N. Sultana, A. Haider and H. Shehnaz, Synthesis and characterization of 3s,5s,7s-adamantan-1-amine complexes with metals of biological interest, *Mod. Chem. Appl.*, 2014, **2**, 120–125.

46 K. Kiranmai, Y. Prashanthi, N. J. P. Subhashini and Shivaraj, Synthesis, characterization and biological activity of metal complexes of 3-amino-5-methyl isoxazole Schiff bases, *J. Chem. Pharm. Res.*, 2010, **2**(1), 375–384.

47 C. Dikio, J. Okoli and F. Mtunzi, Synthesis of new antibacterial agents: hydrazide Schiff bases of vanadium acetylacetonate complexes, *Cogent Chem.*, 2017, **3**, 1336864.

48 H. I. Aljohar, H. A. Ghabbour, M. S. M. Abdelbaky, S. Garcia-Granda and A. A. El-Emam, Crystal structure of N′-[(1E)-(2,6-dichlorophenyl)-methylidene]adamantane-1-carbohydrazide, C18H20Cl2N2O, *Z. Kristallogr. - New Cryst. Struct.*, 2016, **231**, 1037–1039.

49 S. N. Shukla, P. Gaur, S. Jhariya, B. Chaurasia, P. Vaidya, D. Dehariya and M. Azam, Synthesis, characterization, *in vitro* antidiabetic, antibacterial and anticorrosive activity of some Cr(III) complexes of Schiff bases derived from isoniazid, *Chem. Sci. Trans.*, 2018, **7**, 424–444.

50 C. F. Macrae, I. Sovago, S. J. Cottrell, P. T. A. Galek, P. McCabe, E. Pidcock, M. Platings, G. P. Shields, J. S. Stevens, M. Towler and P. A. Wood, Mercury 4.0: from visualization to analysis, design and prediction, *J. Appl. Crystallogr.*, 2020, **53**, 226–235.

51 O. V. Dolomanov, L. J. Bourhis, R. J. Gildea, J. A. Howard and H. Puschmann, OLEX2: a complete structure solution, refinement and analysis program, *J. Appl. Crystallogr.*, 2009, **42**, 339–341.

52 E. Nyawade, F. Ommenya, J. Kinyua and D. Andala, Synthesis, characterization and antibacterial activity of Schiff base, 4-chloro-2-{(E)-[(4-fluorophenyl)imino]methyl} phenol metal (II) complexes, *J. Chem.*, 2020, **2020**, 1–8.

53 Y. Prashanthi and R. Shiva, Synthesis and characterization of transition metal complexes with, *J. Sci. Res.*, 2010, **2**, 114–126.

54 W. Ahmad, S. Khan, K. S. Munawar, A. Khalid and S. Kanwal, Synthesis, characterization and pharmacological evaluation of mixed ligand-metal complexes containing omeprazole and 8-hydroxyquinoline, *Trop. J. Pharm. Res.*, 2017, **16**, 1137–1146.

55 K. S. Munawar, S. Ali, M. N. Tahir, N. Khalid, Q. Abbas, I. Z. Qureshi and S. Shahzadi, Investigation of derivatized Schiff base ligands of 1,2,4-triazole amine and their oxovanadium(IV) complexes: synthesis, structure, DNA binding, alkaline phosphatase inhibition, biological screening, and insulin mimetic properties, *Russ. J. Gen. Chem.*, 2015, **85**, 2183–2197.

56 F. Javed, S. Ali, M. W. Shah, K. S. Munawar, S. Shahzadi, Hameedullah, H. Fatima, M. Ahmed, S. K. Sharma and K. Qanungo, Synthesis, characterization, semi-empirical study, and biological activities of organotin(IV) and transition metal complexes with o-methyl carbonodithioate, *J. Coord. Chem.*, 2014, **67**, 2795–2808.

57 A. Rauf, A. Shah, K. S. Munawar, S. Ali, M. Nawaz Tahir, M. Javed and A. M. Khan, Synthesis, physicochemical elucidation, biological screening and molecular docking studies of a Schiff base and its metal(II) complexes, *Arabian J. Chem.*, 2020, **13**, 1130–1141.

58 Q. Yang, C. Xu, G. C. Han, X. C. Liu, X. D. Jin, B. X. Wang, D. L. Liu and H. H. Hu, Synthesis, characterization, and antibacterial activity of two zinc(II) complexes with Schiff bases from halogenated salicylaldehyde and amantadine, *Russ. J. Coord. Chem.*, 2014, **40**, 634–642.

59 K. S. Munawar, S. Ali, M. N. Tahir, N. Khalid, Q. Abbas, I. Z. Qureshi, S. Hussain and M. Ashfaq, Synthesis, spectroscopic characterization, X-ray crystal structure, antimicrobial, DNA-binding, alkaline phosphatase and insulin-mimetic studies of oxidovanadium(IV) complexes of azomethine precursors, *J. Coord. Chem.*, 2020, **73**, 2275–2300.

60 M. Kaur and R. Kaushal, Synthesis, characterization and α-amylase and α-glucosidase inhibition studies of novel vanadyl chalcone complexes, *Appl. Organomet. Chem.*, 2021, **35**, e6042.

61 H.-Q. Dong, M. Li, F. Zhu, F.-L. Liu and J. B. Huang, Inhibitory potential of trilobatin from lithocarpus polystachyus rehd against α-glucosidase and α-amylase linked to type 2 diabetes, *Food Chem.*, 2012, **130**, 261–266.

62 E. Krieger and G. Vriend, YASARA view—molecular graphics for all devices—from smartphones to workstations, *Bioinformatics*, 2014, **30**, 2981–2982.

63 S. Bilal, M. M. Hassan, M. F. ur Rehman, M. Nasir, A. J. Sami and A. Hayat, An insect acetylcholinesterase biosensor

utilizing WO3/g-C3N4 nanocomposite modified pencil graphite electrode for phosmet detection in stored grains, *Food Chem.*, 2021, **346**, 128894.

64 M. F. Rehman, S. Akhter, A. I. Batool, Z. Selamoglu, M. Sevindik, R. Eman, M. Mustaqeem, M. S. Akram, F. Kanwal, C. Lu and M. Aslam, Effectiveness of natural antioxidants against SARS-CoV-2? insights from the *in silico* world, *Antibiotics*, 2021, **10**, 1011.

65 R. A. Laskowski and M. B. Swindells, LigPlot+: multiple ligand–protein interaction diagrams for drug discovery, *J. Chem. Inf. Model.*, 2011, **1**, 2778–2786.